

Nitro as a novel zinc-binding group in the inhibition of carboxypeptidase A

Si-Hong Wang,^a Shou-Feng Wang,^a Wei Xuan,^a Zong-Hao Zeng,^b
Jing-Yi Jin,^{c,*} Jie Ma^d and Guan Rong Tian^{a,*}

^aDepartment of Chemistry, Yanbian University, Yanji, Jilin 133002, China

^bInstitute of Biophysics, Chinese Academy of Science, Beijing 100871, China

^cKey Laboratory of Organism Functional Factors of the Changbai Mountains of Ministry of Education, Yanbian University, Gongyuan Road 977#, Yanji, Jilin 133002, China

^dCollege of Chemistry and Chemical Engineer, Qiqihaer University, Qiqihaer, Heilongjiang 161006, China

Received 6 January 2008; revised 1 February 2008; accepted 5 February 2008

Available online 8 February 2008

Abstract—2-Substituted 3-nitropropanoic acids were designed and synthesized as inhibitors against carboxypeptidase A (CPA). (*R*)-2-Benzyl-3-nitropropanoic acid showed a potent inhibition against CPA ($K_i = 0.15 \mu\text{M}$). X-ray crystallography discloses that the nitro group well mimics the transition state occurred in the hydrolysis catalyzed by CPA, that is, an *O,O'*-bidentate coordination to the zinc ion and the two respective hydrogen bonds with Glu-270 and Arg-127. Because the nitro group is a planar species, we proposed (*R*)-2-benzyl-3-nitropropanoic acid as a pseudo-transition-state analog inhibitor against CPA.

© 2008 Elsevier Ltd. All rights reserved.

1. Introduction

Zinc proteases are a family of enzymes having a catalytically essential zinc ion at their active sites. These enzymes play key roles in a wide variety of physiological and pathological processes, which are thus the most studied drug design targets, such as angiotensin-converting enzyme (ACE) and matrix metalloproteases (MMPs).^{1,2} The inhibitor design strategy that is widely applied to these pathologically important zinc proteases makes use of a zinc-binding group (ZBG) that can form coordinative bonds to the zinc ion at the active site of the enzymes.^{3–8} The carboxylate or sulfhydryl group are commonly used for such purpose, which are usually lessons from the inhibition of carboxypeptidase A (CPA) as the leading representative of zinc proteases.^{9,10} For example, the carboxylate as the ZBG has been extensively investigated in the inhibition of CPA by 2-benzylsuccinic acid (BSA),¹¹ and then utilized in the

development of enalapril as the ACE inhibitor and Bay-12-9566 as the MMP inhibitor, respectively.²

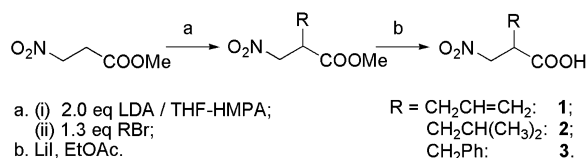
Being an isostere of the carboxylate,¹² the nitro group also shows a variety of coordinative fashions to the metal ions.¹³ Compared to the wide applications of the carboxylate as the ZBG in the inhibition of zinc proteases, the utilization of a nitro group as the ZBG has been rarely explored to the best of our knowledge. We thought that such investigation using CPA as the prototypical enzyme would be of interest as an alternative inhibitor design rationale that can be applied to other zinc proteases of medicinal interests. In the presented paper, we hope to report our studies that involved the introduction of the nitro group as ZBG in the inhibition of CPA.

2. Results and discussion

Three racemic forms of 2-substituted 3-nitropropanoic acids were first synthesized (Scheme 1).¹⁴ Their inhibitory activities against CPA were evaluated and their inhibitory constant (K_i) values are collected in Table 1. It can be found that (*RS*)-2-isobutyl-3-nitropropanoic acid **2** inhibits the CPA-catalyzed hydrolysis more

Keywords: Carboxypeptidase A; Inhibition; Nitro; Zinc-binding group; X-ray crystallography; Transition-state analog inhibitor.

* Corresponding authors. Tel.: +86 4332732286; fax: +86 4332732456 (J.-Y.J.); tel.: +86 4332762289; fax: +86 4332732456 (G.R.T.); e-mail addresses: jjin-chem@ybu.edu.cn; grtn@ybu.edu.cn



Scheme 1. Synthesis of the racemic 2-substituted 3-nitropropanoic acids as inhibitors against CPA.

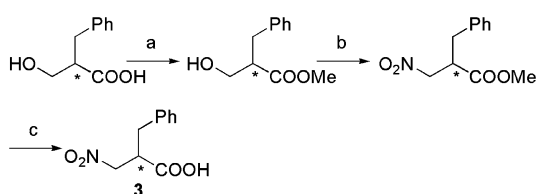
Table 1. Inhibitory constants against CPA

Inhibitor	K_i (μ M)
(<i>RS</i>)- 1	62.6
(<i>RS</i>)- 2	2.08
(<i>RS</i>)- 3	0.79
(<i>R</i>)- 3	0.15
(<i>S</i>)- 3	68
(<i>R</i>)-BSA	0.45 ¹¹

potently than (*RS*)-2-allyl-3-nitropropanoic acid **1**, which should be ascribed to the preference of CPA to the substrate having a large hydrophobic side chain.¹⁵ Introduction of an aromatic ring further augmented the binding affinity of the inhibitors to CPA, which may be resulted from the additional ‘edge-to-face’ interactions of the benzyl side chain of **3** with aromatic enzyme residues.¹⁵

Because (*RS*)-2-benzyl-3-nitropropanoic acid **3** inhibits CPA most potently, we then synthesized the two optically active forms (*R*-, *S*-) of **3** to explore the stereochemistry associated with the inhibition (Scheme 2). The optically pure 2-benzyl-3-hydroxypropanoic acid was obtained according to the literature.¹⁶ Introduction of the nitro group was achieved by the reaction of halogen-NO₂ exchange using Amberlite IRA-900 resin in the nitrite form.¹⁷ Finally, it should be noted that hydrolysis of 3-nitropropanoic acid methyl ester under the acidic or basic conditions failed. The needed carboxylic acids can be obtained through treatment of the ester with lithium iodide in refluxing anhydrous ethyl acetate, which has been previously reported to be efficacious for ester dealkylation of compounds having an X=O group (X = C or S) at the γ -position to the ester moiety.^{18,19}

Consistent to the L-specificity of CPA, (*R*)-**3** is the more potent inhibitor of CPA than the corresponding *S*-form. Especially, the K_i value of (*R*)-**3** against CPA is 0.15 μ M, which is about threefold more potent than (*R*)-BSA ($K_i = 0.45 \mu$ M).¹¹



Scheme 2. Synthesis of both optically pure 2-benzyl-3-nitropropanoic acids. Reagents: (a) HCL-MeOH; (b) i—MeSO₂Cl, DMAP; ii—LiBr; iii—Amberlite IR-900, NaNO₂; (c) LiI, EtOAc.

To explore the binding mode of (*R*)-**3** at the active site of CPA,²⁰ CPA-(*R*)-**3** crystals for X-ray diffraction were then obtained by soaking the enzyme crystals into the solution containing racemic **3** and determined at a resolution of 1.5 Å (PDB ID code: 2RFH). The final model including all residues of CPA and (*R*)-**3** was refined in the 38.42–1.70 Å (Table 2). Figure 1 depicts the stereo-view of the difference electron density in the region of the active site of CPA that is occupied by (*R*)-**3**. Distances of important interactions between CPA and (*R*)-**3** in the complex are listed in Table 3.

The X-ray crystallographic studies disclosed the following main structural information. Firstly, it is found that (*R*)-**3** occupies the S1' subsite of CPA where it makes the expected interactions: the benzyl moiety resides in the

Table 2. Data collection and refinement statistics for the CPA-(*R*)-**3** complex

Space group	$P2_1$
Unit cell	
a, b, c (Å)	42.30, 62.70, 48.97
α, β, γ (deg)	90.00, 96.99, 90.00
Resolution range (Å)	38.42–1.70
Number of unique reflections	27,657
Overall completeness (%)	98.7
R_{merge} (%) ^a	4.5
R factor ^b	22.6
rms deviations ^c	
Bonds (Å)	0.013
Angles (deg)	1.3
Dihedrals (deg)	14.1

^a $R_{\text{merge}} = \frac{\sum_i \sum_h \|F_{hi}\| - \langle |F_h| \rangle}{\sum_i \sum_h \|F_{hi}\|}$, $|F_{hi}|$ = scaled structure factor for reflection h in data set i , $\langle |F_h| \rangle$ = average structure factor for reflection h calculated from replicate data.

^b R factor, $R = \frac{\sum |F_o| - |F_c|}{\sum |F_o|}$; $|F_o|$ and $|F_c|$ are the observed and calculated structure factors, respectively.

^c rms: root mean square.

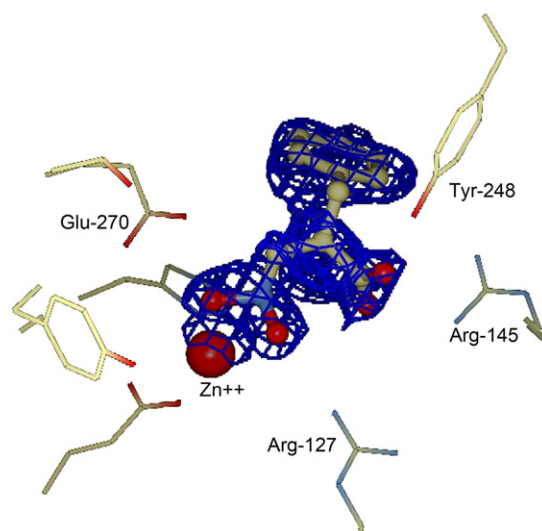


Figure 1. Difference electron density map for CPA-(*R*)-**3** complex generated with Fourier coefficient $|F_o| - |F_c|$ phases calculated from the final model omitting the bound inhibitor.

Table 3. Selected CPA-(*R*)-3 interactions

Atom in (<i>R</i>)-3	Enzyme residue	Separation (Å)
O ¹	Arg-145 guanidinium N ¹	2.99
O ²	Arg-145 guanidinium N ²	2.63
O ¹	Tyr-248 phenolic O	3.90
O ³	Zn ²⁺	2.10
O ⁴	Zn ²⁺	3.06
O ³	Arg-127 guanidinium N ¹	4.89
O ⁴	Arg-127 guanidinium N ²	2.87
O ³	Glu-270 carboxylate O ¹	2.60
O ⁴	Glu-270 carboxylate O ²	4.49

hydrophobic pocket and the carboxylate makes a salt link with the guanidinium group of Arg-145. Tyr-248 is found in the ‘so-called’ down position, which is responsible to the formation of the hydrophobic pocket. Such binding modes are commonly observed in X-ray crystal structures of CPA-inhibitor complexes.¹⁵ Secondly, the nitro group of (*R*)-3 acts as an asymmetric bidentate ligand of the zinc ion in an *O,O'*-chelation mode (2.10 and 3.06 Å). In this sense, the nitro group should be reasonably regarded as a new ZBG. Finally, the two oxygen atoms (O³ and O⁴) of the nitro moiety in (*R*)-3 are engaged in hydrogen bonding with one of the carboxylate oxygen atoms in Glu-270 and one of the guanidinium nitrogen atoms in Arg-127 with the distances of 2.60 and 2.87 Å, respectively. In the CPA-(*R*)-BSA complex,²¹ the similar hydrogen bond between the inhibitor and Glu-270 could be observed but the hydrogen bond with Arg-127 is missing. Therefore, the more potent inhibition exhibited by (*R*)-3 than (*R*)-BSA could be reasonably ascribed to the additional hydrogen bond with Arg-127 in the CPA-(*R*)-3 complex (Fig. 2).

It is interesting to discuss the inhibition type shown by (*R*)-3 against CPA. It has been generally accepted that the transition state in the CPA-catalyzed hydrolysis is structurally featured by the tetrahedral carbon with the *gem*-diolate oxygens stabilized by chelation to the zinc ion and two respective hydrogen bonds with Glu-270 and Arg-127 (Fig. 2a).¹⁵ For the typical transition-state analog inhibitor against CPA, *O*-[[*(1R)*-[[*N*-phenylmethoxycarbonyl]-L-alanyl]amino]ethyl]hydroxyphosphinyl]-L-3-phenyllactate, the salient structural features are coordination of the phosphinyl moiety to the zinc and Arg-127 and a short distance between a phosphinyl

oxygen and a glutamate oxygen of Glu-270 (Fig. 2b).²² In spite of being not a tetrahedron species, the nitrite in CPA-(*R*)-3 complex exhibited all above the structurally essential features of the transition state (Fig. 2d).²³ Therefore, we suggest (*R*)-3 as a pseudo-transition-state analog inhibitor for CPA.

3. Conclusion

In conclusion, we successfully introduced the nitro group as a new ZBG to the inhibition of CPA. X-ray crystallography of CPA-(*R*)-3 complex disclosed its *O,O'*-bidentate chelation to the zinc ion at the active site of CPA. Although the nitro group is not a tetrahedron species, it also showed the similar binding modes as transition-state analog. We then proposed it as a new pseudo-transition-state analog inhibitor for CPA.

4. Experimental

4.1. Materials and methods

All chemicals were purchased from Aldrich and used as received without further purification. Flash chromatography was performed with 100–200 mesh silica gel (Qingdao, China) and thin-layer chromatography (TLC) was carried out on silica coated glass sheets (Qingdao silica gel 60 F-254). Melting points were taken on a Thomas–Hoover capillary melting point apparatus and uncorrected. ¹H nuclear magnetic resonance (NMR) and ¹³C NMR spectra were recorded with a Bruker AV 300 (300 MHz) instrument using tetramethylsilane as the internal standard. IR spectra were recorded on a Perkin-Elmer 1300 FT-IR spectrometer. High-resolution mass spectra were taken on a Shimadzu GC–MS–QP2010. Elemental analyses were performed at Changchun Institute of Applied Chemistry, Chinese Academy of Sciences, Changchun, China.

CPA was purchased from Sigma Chemical Co. (Allan form, twice crystallized from bovine pancreas, aqueous suspension in toluene) and used without further purification for kinetic assays. Lithium chloride and Hepes were obtained from Sigma. *O*-(*trans*-*p*-chlorocinnamoyl)-L-β-phenyllactate (Cl-CPL) was used as the substrate in the kinetic study.²⁴ All solutions for kinetic study were prepared by dissolving in doubly distilled and deionized water. CPA stock solutions were prepared by dissolving CPA in 0.05 M Tris/0.5 M NaCl, pH 7.5, buffer solution and their concentrations were estimated from the absorbance at 278 nm ($\epsilon_{278} = 64,200$). The stock assay solutions were filtered (GHP Acrodisc syringe filter, pore size 0.2 μm) before use. Perkin-Elmer HP 8453 UV–Vis spectrometer was used for UV absorbance measurements.

4.2. Synthesis

4.2.1. General procedure for the synthesis of (*RS*)-2-substituted 3-nitropropanoic acid. To a solution of lithium diisopropylamide (LDA, 2.3 equiv) and hexam-

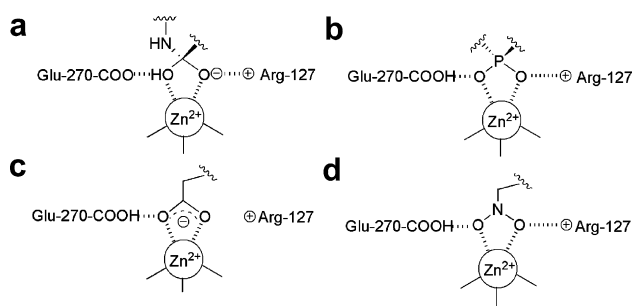


Figure 2. Schematic representation of the binding mode of (a) the occurred tetrahedron intermediate in the catalysis of the peptide substrate; (b) the phosphate-based transition-state analog inhibitor; (c) 2-benzylsuccinic acid; and (d) 2-benzyl-3-nitropropanoic acid to CPA.

ethylphosphorous triamide (HMPA, 5.0 equiv) in THF at $-78\text{ }^{\circ}\text{C}$ was added 3-nitropropanoic methyl ester (1.0 equiv). After stirring for 1 h, the corresponding halides (1.25 equiv) were then added. The solution was kept stirring at the same temperature for 5 h. The reaction was quenched by addition of acetic acid (1.0 equiv) followed by distilled water. After warmed to room temperature, the solution was then diluted by water and extracted by diethyl ether for three times. The combined organic layer was washed with brine and then dried over anhydrous MgSO_4 . Evaporation under reduced pressure provided an oil, which was then purified by column chromatography (*n*-hexane/EtOAc = 5:1) to give the corresponding methyl ester.

To an anhydrous solution of ethyl acetate containing the above methyl ester (1.0 equiv) was added lithium iodide (7.0–8.0 equiv). The resulting mixture was heated under reflux for 24 h under N_2 . After cooling to room temperature, the reaction mixture was treated with water and then acidified to pH 1.0 with 10% citric acid solution. After extracted with ethyl acetate, the combined organic layer was washed with saturated $\text{Na}_2\text{S}_2\text{O}_3$ solution and then dried over anhydrous MgSO_4 . Evaporation under reduced pressure provided an oil, which was then purified by column chromatography to give the needed acids.

(*RS*)-1: IR (KBr): 1364, 1569, 1738, 3460 cm^{-1} . ^1H NMR (300 MHz, CDCl_3) δ : 2.28–2.49 (m, 2H), 3.20–3.39 (m, 1H), 4.57 (dd, $J = 5.6, 10.2$ Hz, 1H), 4.71 (dd, $J = 5.6, 10.2$ Hz, 1H), 5.11–5.18 (m, 2H), 5.76–5.85 (m, 1H). ^{13}C NMR (75 MHz, CDCl_3) δ : 33.00, 42.30, 74.17, 117.41, 133.54, 173.94. HRMS calcd for $\text{C}_6\text{H}_9\text{NO}_4$: 159.0532. Found: 159.0530.

(*RS*)-2: IR (KBr) 1363, 1571, 1738, 3457 cm^{-1} . ^1H NMR (300 MHz, CDCl_3) δ : 0.98 (d, $J = 6.1$ Hz, 6H), 1.37–1.43 (m, 1H), 1.63–1.73 (m, 2H), 3.26–3.30 (m, 1H), 4.43 (dd, $J = 4.8, 9.8$ Hz, 1H), 4.71 (dd, $J = 4.8, 9.8$ Hz, 1H), 8.68 (s, 1H). ^{13}C NMR (75 MHz, CDCl_3) δ : 22.06, 22.32, 25.65, 37.99, 40.98, 75.05, 178.19. HRMS calcd for $\text{C}_7\text{H}_{13}\text{NO}_4$: 175.0845. Found: 175.0844.

(*RS*)-3: mp 70–71 $^{\circ}\text{C}$. IR (KBr): 3429, 1718, 1016 cm^{-1} ; ^1H NMR (300 MHz, CDCl_3) δ : 2.88 (dd, $J = 5.4, 14.0$ Hz, 1H), 3.41 (dd, $J = 5.4, 14.0$ Hz, 1H), 3.30–3.70 (m, 1H), 3.90 (dd, $J = 5.2, 12.6$ Hz, 1H), 4.66 (dd, $J = 5.2, 12.6$ Hz, 1H), 7.19–7.39 (m, 5H), 9.22 (br, 1H). ^{13}C NMR (75 MHz, CDCl_3) δ : 34.78, 44.31, 73.52, 127.57, 128.87, 129.11, 136.08, 178.01. Anal. $\text{C}_{10}\text{H}_{11}\text{NO}_4$ requires C, 57.41; H, 5.30; N, 6.70. Found: C, 57.48; H, 5.33; N, 6.65.

4.2.2. General procedure for the synthesis of the optically active 2-benzyl-3-hydroxypropanoic acid methyl ester.

To an ice-chilled stirred solution of 2-benzyl-3-hydroxypropanoic acid (1.0 equiv) in MeOH (20 mL) was added acetyl chloride (2 mL). The mixture was stirred for 24 h at room temperature, and then evaporated under reduced pressure. The residue was dissolved in ethyl acetate (30 mL) followed by neutralization with

aqueous NaHCO_3 solution. The organic layer was washed with brine and then dried over anhydrous MgSO_4 . Evaporation under reduced pressure provided an oil, which was then purified by column chromatography (*n*-hexane/EtOAc = 5:1) to give the corresponding methyl ester as an oil. Yield: 86%. IR (KBr): 3303, 1735 cm^{-1} . ^1H NMR (300 MHz, CDCl_3) δ : 2.18 (t, $J = 9.2$ Hz, 1H), 2.88 (m, 2H), 3.03 (dd, $J = 9.2, 16.9$ Hz, 1H), 3.70 (s, 3H), 3.65–3.80 (m, 2H), 7.19–7.35 (m, 5H). ^{13}C NMR (75 MHz, CDCl_3) δ : 34.41, 49.24, 51.85, 62.24, 126.54, 128.52, 128.91, 138.56, 175.11.

(*S*)-2-Benzyl-3-hydroxypropanoic acid methyl ester: $[\alpha]_{\text{D}}^{23} +39.3^{\circ}$ (c 0.41, CH_3OH). HRMS calcd for $\text{C}_{11}\text{H}_{14}\text{O}_2$: 178.0944. Found: 178.0943.

(*R*)-2-Benzyl-3-hydroxypropanoic acid methyl ester: $[\alpha]_{\text{D}}^{23} = -38.6^{\circ}$ (c 0.47, CH_3OH), HRMS calcd for $\text{C}_{11}\text{H}_{14}\text{O}_2$: 178.0944. Found: 178.0943.

4.2.3. General procedure for the synthesis of the optically active 2-benzyl-3-nitropropanoic acid methyl ester.

To 5 mL solution of CH_2Cl_2 containing the optically active 2-benzyl-3-hydroxypropanoic acid methyl ester (1.0 equiv), dimethylaminopyridine (0.05 equiv) and pyridine (2.0 equiv) at 0 $^{\circ}\text{C}$, a solution of methanesulfonyl chloride (2.0 equiv) in CH_2Cl_2 (1 mL) were added. After standing at room temperature overnight, the reaction mixture were then poured into 20 mL 10% HCl followed by extraction with ethyl acetate (3 \times 15 mL). The combined organic layer was washed with aqueous NaHCO_3 and brine, and then dried over anhydrous MgSO_4 . Evaporation under reduced pressure gave an oil, which was then purified by column chromatography (silica gel, *n*-hexane/EtOAc = 5:1) to yield the needed mesylate.

A solution of tetrahydrofuran containing the above mesylate and anhydrous lithium bromide (2.0 equiv) was kept stirring at room temperature. Completion of the reaction was ensured by the TLC detection. After addition of ethyl acetate, the organic layer was washed with water and then dried over anhydrous MgSO_4 . Evaporation under reduced pressure gave the crude product, which was then purified by column chromatography (silica gel, *n*-hexane/EtOAc = 10:1) to yield the bromide.

Amberlite IRA-900 in the nitrite form (1.5 g) was added to a solution of benzene containing the above bromide (112 mg, 0.439 mmol). The resulting slurry was kept stirring at 20 $^{\circ}\text{C}$ for 36 h. After filtration, the filtrate was evaporated under reduced pressure to give a yellow oil. Purification by column chromatography (silica gel, *n*-hexane/EtOAc = 5:1) to yield the product as an oil. Yield: 33 %. IR (KBr): 3304, 1733 cm^{-1} . ^1H NMR (300 MHz, CDCl_3) δ : 2.84 (dd, $J = 9.0, 14.0$ Hz, 1H), 3.16 (dd, $J = 8.9, 14.0$ Hz, 1H), 3.40–3.60 (m, 1H), 3.75 (s, 3H), 4.35 (dd, $J = 4.4, 14.6$ Hz, 1H), 4.68 (dd, $J = 4.3, 14.6$ Hz, 1H), 7.16–7.38 (m, 5H). ^{13}C NMR (75 MHz, CDCl_3) δ : 35.09, 44.49, 52.51, 74.06, 127.38, 128.84, 128.97, 136.40, 172.03.

(*S*)-2-Benzyl-3-nitropropanoic acid methyl ester. $[\alpha]_{\text{D}}^{23}$ -7.8 (c 0.26, CH₃OH). HRMS calcd for C₁₁H₁₃NO₃: 207.0895. Found: 207.0894.

(*R*)-2-Benzyl-3-nitropropanoic acid methyl ester. $[\alpha]_{\text{D}}^{23}$ $+8.1$ (c 0.24, CH₃OH). HRMS calcd for C₁₁H₁₃NO₃: 207.0895. Found: 207.0894.

4.2.4. Synthesis of the optically active 2-benzyl-3-nitropropanoic acid. The procedures are similar as described in the general procedures of hydrolysis of the methyl esters containing nitro group.

(*S*)-**3**: mp 70–71 °C. $[\alpha]_{\text{D}}^{25}$ -4.3° (c 0.34, CH₃OH). HRMS calcd for C₁₀H₁₁NO₄: 209.0689. Found: 209.0688. Anal. C₁₀H₁₁NO₄ requires C, 57.41; H, 5.30; N, 6.70. Found: C, 57.44; H, 5.31; N, 6.94.

(*R*)-**3**: mp 70–71 °C. $[\alpha]_{\text{D}}^{25}$ $+4.5^{\circ}$ (c 0.33, CH₃OH). HRMS calcd for C₁₀H₁₁NO₄: 209.0689. Found: 209.0688. Anal. C₁₀H₁₁NO₄ requires C, 57.41; H, 5.30; N, 6.70. Found: C, 57.58; H, 5.33; N, 6.65.

4.3. Determination of K_i value

The enzyme stock solution was added to a solution containing Cl-CPL (final concentrations: 50 and 100 μM) and inhibitor (five different final concentrations in the range of 0.5–2.0 K_i) in 0.05 M Tris/0.5 M NaCl, pH 7.5, buffer (1 mL cuvette), and the change in absorbance at 320 nm was measured immediately. The final concentration of CPA was 20 nM. Initial velocities were then calculated from the linear initial slopes of the change in absorbance where the amount of substrate consumed was less than 10%. The K_i values were then estimated from the semireciprocal plot of the initial velocity versus the concentration of the inhibitor according to the method of Dixon.²⁵

4.4. X-ray crystallography

CPA was washed three times with water to remove toluene used in packaging and then dissolved in 1.2 M LiCl. After centrifugation, the enzyme solution was then diluted to 10–15 mg/mL with a buffer solution of 1.2 M LiCl, 25 mM Tris, pH 7.5. An aliquot of this solution was then pipetted into a 100 μL glass dialysis button. A 7 kDa molecular weight cutoff membrane, which was pre-washed by doubly distilled and deionized water followed by equilibrated in 0.15 M LiCl, was placed over the button and secured with a rubber O-ring. The button was then dialyzed against 0.2 M LiCl, 25 mM Tris, pH 7.5, and at 4 °C. Crystals appeared after about 4 days on the bottom and edges of the well. The crystals were then crosslinked using a buffer solution containing 0.15 M LiCl and 0.02% (v/v) glutaraldehyde for 90 min. The crystals were then transferred to a soaking solution of the same buffer containing 2 mM racemic **3** and stored for 17 days in a cold room (4 °C) before data collection. Single crystals grew in the P_{21} space group with one molecule in the asymmetric unit. Crystallographic data were collected using a Rigaku RA-Micro 7 Desktop Rotating Anode X-ray Generator with a Cu target

operating at 40 kV × 20 mA and R -Axis IV⁺⁺ imaging-plate detector at a wavelength of 1.5418 Å. A 0.5 mm collimator was used to keep the whole crystal bathed in the X-ray beam. A total of 360 images with 1.0 oscillation were collected. The collected intensities were indexed, integrated, corrected for absorption, scaled and merged using HKL2000. Diffraction images were processed with the CCP4 program suite. The structure of the native CPA (PDB code: 5CPA) was used as the starting model. Model refinement was carried out with the COOT program and the REFMAC 5.2. Water molecules were added to the model with the program CCP-4. The inhibitor model was included in the last stage of the refinement.

Acknowledgment

The work was financially supported by the Science and Technology Committee of Jilin Province (No. 20060568) and the Open Project Program of Key Laboratory of Organism Functional Factors of the Changbai Mountains of Ministry of Education, Yanbian University, China.

References and notes

- Babine, R. E.; Bender, S. L. *Chem. Rev.* **1997**, *97*, 1359.
- Leung, D.; Abbenante, G.; Fairlie, D. P. *J. Med. Chem.* **2000**, *43*, 305.
- Jacobsen, F. E.; Lewis, J. A.; Cohen, S. M. *J. Am. Chem. Soc.* **2006**, *128*, 3156.
- Rush, T. S.; Powders, R. *Curr. Top. Med. Chem.* **2004**, *4*, 1311.
- Tekeste, T.; Vahrenkamp, H. *Inorg. Chem.* **2006**, *45*, 10799.
- Tekeste, T.; Vahrenkamp, H. *Eur. J. Inorg. Chem.* **2006**, *24*, 5158.
- Jacobsen, F. E.; Cohen, S. M. *Inorg. Chem.* **2004**, *43*, 3038.
- He, H.; Puerta, D. T.; Cohen, S. M.; Rodgers, K. R. *Inorg. Chem.* **2005**, *44*, 7431.
- Lipscomb, N. W.; Sträter, N. *Chem. Rev.* **1996**, *96*, 2375.
- Whittaker, M.; Floyd, C. D.; Brown, P.; Gearing, A. J. H. *Chem. Rev.* **1999**, *99*, 2735.
- Byers, L. D.; Wolfenden, R. *Biochemistry* **1973**, *12*, 2070.
- Sun, F.; Huo, X.; Zhai, Y. J.; Wang, A. J.; Xu, J. X.; Su, D.; Bartlam, M.; Rao, Z. H. *Cell* **2005**, *121*, 1043.
- Hitchman, M. A.; Rowbottom, G. L. *Coord. Chem. Rev.* **1982**, *42*, 55–132.
- Seebach, D.; Henning, R.; Mukhopadyyay, T. *Chem. Ber.* **1982**, *115*, 1705.
- Christianson, D. W.; Lipscomb, W. M. *Acc. Chem. Res.* **1989**, *22*, 62.
- Lee, H. S.; Park, J. D.; Kim, D. H. *Bull. Korean Chem. Soc.* **2003**, *24*, 467.
- Gelbard, G.; Colonna, S. *Synthesis* **1977**, *1977*, 113.
- Fisher, J. W.; Trinkle, K. L. *Tetrahedron Lett.* **1994**, *35*, 2505.
- Jin, J.-Y.; Tian, G. R.; Kim, D. H. *Bioorg. Med. Chem.* **2003**, *11*, 4377.
- We also performed the computer simulated automated docking studies using the widely distributed molecular docking software, AutoDock 4.0.²⁶ Although it remains as a challenge to predict metal–ligand interactions with a satisfied accuracy by means of docking programs, recent

progress on molecular modelling provided some examples to evaluate the metal binding interactions using AutoDock program.²⁷ In our results, the nitro group do coordinate to the zinc ion at the active site of CPA in an *O,O'*-bidentate fashion, but the hydrogen bonds are missing.

21. Mangani, S.; Carloni, P.; Orioli, P. *J. Mol. Biol.* **1992**, *223*, 573.
22. Kim, H.; Lipscomb, W. N. *Biochemistry* **1990**, *29*, 5546.
23. For the other transition-state analog inhibitors for CPA, see examples: (a) Cappalonga, A. M.; Alexander, R. S.; Christianson, D. W. *J. Biol. Chem.* **1992**, *267*, 19192; (b) Park, J.-D.; Kim, D. H.; Kim, S.-J.; Woo, J.-R.; Ryu, S.-E. *J. Med. Chem.* **2002**, *45*, 5295.
24. Suh, J.; Kaiser, E. T. *J. Am. Chem. Soc.* **1976**, *98*, 1940.
25. Dixon, M. *Biochem. J.* **1953**, *55*, 170.
26. Morris, G. M.; Goodsell, D. S.; Halliday, R. S.; Hart, W. E.; Belew, R. K.; Olson, A. J. *J. Comput. Chem.* **1998**, *19*, 1639.
27. Chen, D.; Menche, G.; Power, T. D.; Sower, L.; Peterson, J. W.; Schein, C. H. *Proteins* **2007**, *67*, 593.